Thiol Oxidation

DOI: 10.1002/anie.201309302

Flavoenzyme-Catalyzed Formation of Disulfide Bonds in Natural Products**

*Daniel H. Scharf, Michael Groll, Andreas Habel, Thorsten Heinekamp, Christian Hertweck, Axel A. Brakhage, and Eva M. Huber**

Abstract: *Nature provides a rich source of compounds with diverse chemical structures and biological activities, among them, sulfur-containing metabolites from bacteria and fungi. Some of these compounds bear a disulfide moiety that is indispensable for their bioactivity. Specialized oxidoreductases such as GliT, HlmI, and DepH catalyze the formation of this disulfide bridge in the virulence factor gliotoxin, the antibiotic holomycin, and the anticancer drug romidepsin, respectively. We have examined all three enzymes by X-ray crystallography and activity assays. Despite their differently sized substrate binding clefts and hence, their diverse substrate preferences, a unifying reaction mechanism is proposed based on the obtained crystal structures and further supported by mutagenesis experiments.*

Disulfide bridges are known as integral structural components of peptides and proteins. Yet, disulfide moieties are also found in various natural products where they play a pivotal role in determining biological activity. Important examples are the broad-spectrum antibiotic holomycin (**1**; Scheme 1) from *Streptomyces clavuligerus*, the FDA-approved anticancer depsipeptide romidepsin (**2**) from *Chromobacterium violaceum*, and gliotoxin (**3**) from the human pathogenic fungus *Aspergillus fumigatus*. Gliotoxin has been implicated as virulence factor in invasive aspergillosis, a frequent cause of death in immunosuppressed patients,[1] and it is the most prominent representative of epipolythiodioxopiperazines (ETPs). The toxicity of ETPs is linked to their reactive epidithio moiety,[2] which inactivates essential sulfur-containing proteins by conjugation, disturbs the intracellular redox equilibrium, and generates reactive oxygen species.[3]

In the past years the biosynthesis of **3** has been studied genetically and biochemically.[4] The sulfur moieties are introduced to the diketopiperazine core[5] by the addition of glutathione (GSH)[6] and its sequential degradation to the free thiol precursor (**4**).[7] A flavin adenine dinucleotide (FAD)-dependent oxidoreductase, termed GliT, finally oxidizes **4** to the disulfide-containing gliotoxin (**3**), thereby conferring resistance of the fungus to its own toxin.[8] It is very conceivable that GliT-type enzymes catalyze the final biosynthesis step of all ETPs.[8a]

Oxidoreductases closely related to GliT have been found in bacteria[9] and fungi and can be grouped in three distinct clades according to their prototypes TrxR, DepH, and HlmI (Figure S1A in the Supporting Information). The TrxR family is crucial for intracellular redox regulation,[10] while the HlmI and DepH groups presumably oxidize small molecules (Scheme 1). Specifically, HlmI is involved in the biosynthesis of **1**[9a] and DepH installs the disulfide bridge in **2**.[9b] The four clades of oxidoreductases share the catalytically active Cys-X-X-Cys motif, but their substrate specificities are fairly diverse. In order to shed light on the differences between these enzyme families and to elucidate their reaction mechanisms, we solved the X-ray structures of GliT from *A. fumigatus* (1.9 Å; R_{free} 22.2%) as well as of the two closely related bacterial oxidoreductases HlmI from *S. clavuligerus* (1.6 Å; R_{free} 15.9%) and DepH from *C. violaceum* (1.9 Å; R_{free} 19.9%), respectively (Table S1 in the Supporting Information). All three enzymes are homodimers and display the typical fold of thioredoxin reductases with one FAD molecule bound per monomer, [rmsd C_α(HlmI/DepH/GliT) < 2.2 Å; rmsd C_α(HlmI/DepH/GliT/TrxR) < 6.6 Å; Figure 1A; Figures S2 and S3 and Table S2 in the Supporting Information).[11] Each monomer comprises one FAD and one nicotinamide adenine dinucleotide phosphate ($NADP^+$/NADPH) binding domain that adopt the β-α-β-α-β Rossman fold and that are connected by an antiparallel β-sheet. At the primary sequence level the FAD recognition site is split by the $NADP^+$/NADPH binding domain (Figure S1B in the Supporting Information). The FAD-binding domains, in particular the helices H1 and H2 and their connecting loop, form a dimerization interface of 2200 $Å^2$ to 2750 $Å^2$. In contrast to DepH,[9b] the $NADP^+$/NADPH binding sites of GliT and HlmI are assumed to be nonfunctional, as both use O_2 instead of $NADP^+$ as a cosubstrate and terminal electron acceptor.[8a,9a] The $NADP^+$/NADPH binding domains also harbor

[*] Prof. Dr. M. Groll, Dr. E. M. Huber
Center for Integrated Protein Science at the Department Chemistry
Chair of Biochemistry, Technische Universität München
Lichtenbergstrasse 4, 85748 Garching (Germany)
E-mail: eva.huber@mytum.de
Dr. D. H. Scharf, Dr. A. Habel, Dr. T. Heinekamp,
Prof. Dr. C. Hertweck, Prof. Dr. A. A. Brakhage
Departments of Molecular and Applied Microbiology and Biomolecular Chemistry, Leibniz Institute for Natural Product Research and Infection Biology, HKI, and Friedrich Schiller University Jena
Beutenbergstrasse 11a, 07745 Jena (Germany)

[**] We thank M. Gersch and Prof. Dr. S. A. Sieber (TUM) for MS measurements, S. Fricke and C. Schult (HKI) for technical support, and P. Hortschansky for scientific support. We thank the staff of the beamline X06SA at the Paul Scherrer Institute, Swiss Light Source (Villigen, Switzerland) for assistance during data collection. This work was supported by the "Pakt für Forschung und Innovation" of the Free State of Thuringia and the BMBF, and the International Leibniz Research School for Biomolecular and Microbial Interactions (ILRS), as part of the Jena School for Microbial Communication, an excellence graduate school.

Supporting information for this article is available on the WWW under http://dx.doi.org/10.1002/anie.201309302.

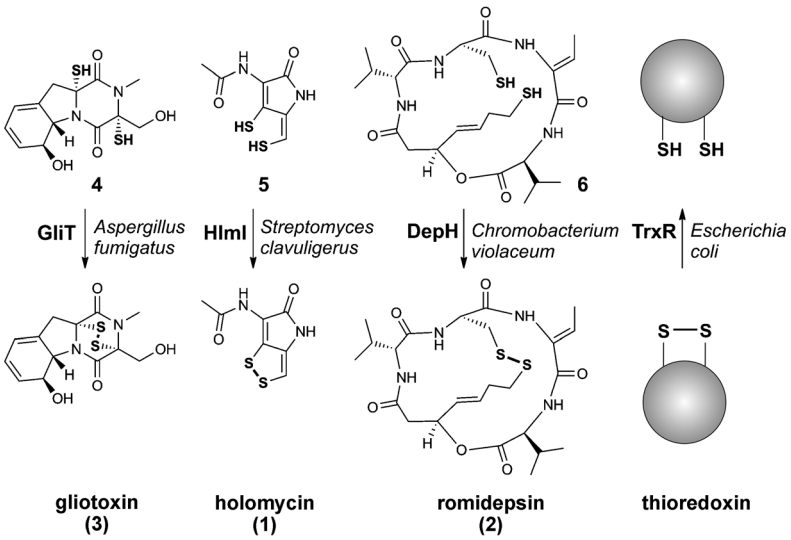

Scheme 1. Specialized oxidases install transannular disulfide bridges in fungal and bacterial secondary metabolites. The structurally related bacterial TrxR catalyzes the reduction of a disulfide bond in thioredoxin.

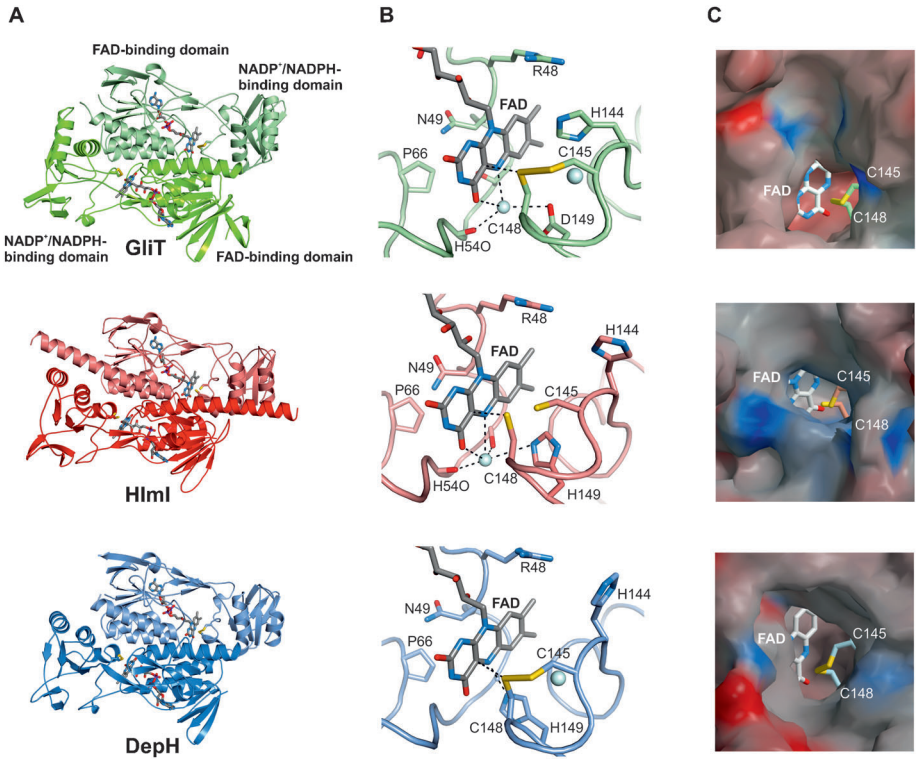

Figure 1. X-ray structures of GliT, HlmI, and DepH. A) Ribbon illustration of the enzymes with their cofactor FAD and their catalytic cysteines depicted as stick models. B) Enlargment of the active site of the respective enzymes. Residues (except for Thr/Ser/Ala52) are labeled according to the sequence alignment provided in Figure S1B. Water molecules are shown as light blue spheres; black dotted lines indicate important interactions/distances. In GliT and HlmI a water molecule near the N5 atom of FAD functions as a proton donor (distance: 2.9–3.3 Å); in DepH, His149 assumes this function (distance: 3.0 Å). The water molecule next to Cys145 in GliT and DepH is oriented by the helix dipole H4 of the CXXC box and replaced in HlmI by GSH (Figure S5). The distance between the electron-donating Cys148S and the electron-accepting $C4^{\alpha}$ atom of FAD in the GSH-bound HlmI is shorter (3.1 Å) than in the apo structures of GliT and DepH (3.4 Å). C) Connolly surface representations of the substrate-binding clefts depict their difference in size. Positive and negative electrostatic surface potentials are contoured from −30 kT/e (red) to 30 kT/e (blue). The active-site cysteines and the FAD moiety were removed for surface calculations.

the conserved Cys145-X-X-Cys148 motif (CXXC; numbering according to Figure S1B in the Supporting Information), a hallmark of numerous oxidoreductases.[11] Connolly surface illustrations reveal that in each of the two protein subunits the active cysteines are located at the bottom of a pronounced substrate-binding pocket formed by the dimer interface (Figure 1 A and C).

In line with results obtained for DepH and HlmI,[9] our activity assays with GliT mutants demonstrate that both catalytic cysteines are essential for enzymatic activity in vitro (Figure 2 A). Moreover, *A. fumigatus* strains carrying mutations in the CXXC box show increased sensitivity towards gliotoxin, similar to the Δ*gliT* knockout (Figure 2 C), indicating that this motif is crucial for GliT-mediated self-resistance. The helical conformation of the CXXC box enables the formation of a disulfide bridge between Cys145 and Cys148. Likewise in TrxR, the active-site cysteines of GliT, HlmI, and DepH stack against the *Re* side of the isoalloxazine ring. However, in GliT, HlmI, and DepH the disulfide bond is perpendicular to the flavin system. This orientation of the catalytic disulfide resembles that in glutathione reductases,[12] but contrasts with the more parallel positioning in TrxR (Figure S2C).[11] Due to its close proximity to the $C4^{\alpha}$ atom of the prosthetic group (3.1–3.5 Å), Cys148 is supposed to mediate electron transfer to the FAD cofactor during catalysis, whereas Cys145, located more distal from the FAD (5.3–5.8 Å), forms the mixed disulfide with the substrate. Such a differential reactivity of the catalytic cysteines has also been observed for dihydrolipoamide dehydrogenase, the E3 component of the pyruvate dehydrogenase complex.[13]

The crystal structures of GliT, HlmI, and DepH allowed us to propose the following reaction mechanism for thiol oxidation in natural compounds, which is analogous to that for disulfide formation in proteins[14] (Figure 3): Deprotonation of one of the substrate's thiols creates a reactive thiolate anion that nucleophilically attacks the enzyme's catalytic disulfide. Hereby, the substrate becomes

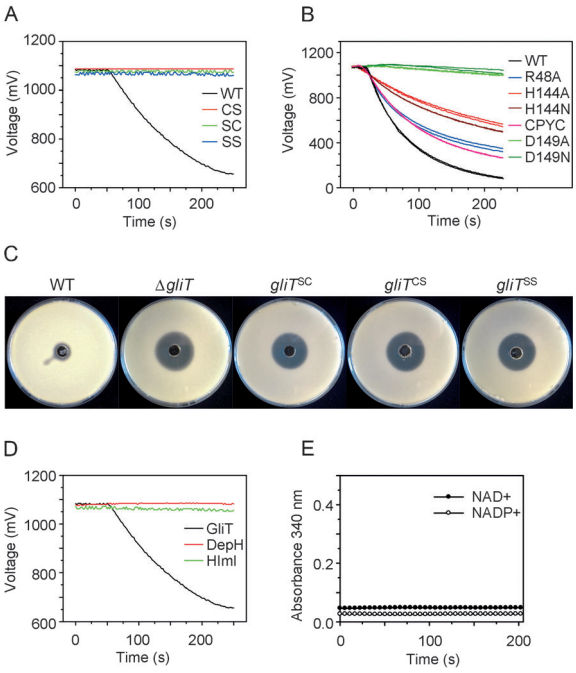

Figure 2. Biochemical characterization of GliT, HlmI, and DepH. A) Wild-type GliT oxidizes **4** under the consumption of O_2; mutations in the CXXC motif prevent enzymatic activity. B) Substrate conversion by various GliT mutants; for example, the CLFC motif was exchanged for the CPYC box from HlmI and DepH. C) Sensitivity of *A. fumigatus* towards **3** is strongly increased when GliT is absent or nonfunctional due to mutation of the active-site cysteines. D) In contrast to GliT, HlmI and DepH do not accept **4** as a substrate in an O_2-depletion assay. E) DepH is not able to oxidize **4** in the presence of NAD^+ or $NADP^+$.

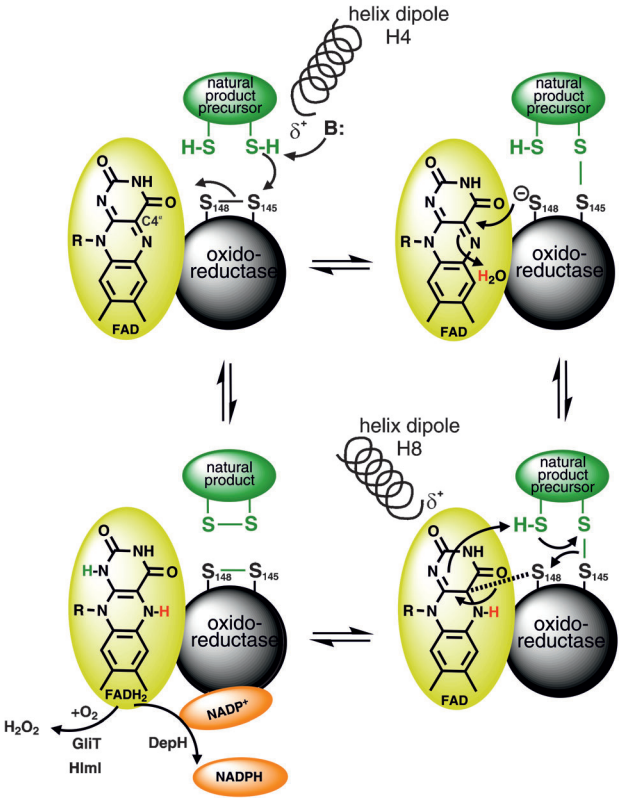

Figure 3. Proposed reaction mechanism for the oxidation of **4**–**6** by the oxidoreductases GliT, HlmI, and DepH, respectively.

covalently linked to Cys145 of the enzyme and a thiolate at Cys148 is formed, which forms a transient charge-transfer complex with the $C4^{\alpha}$ atom of the electron-deficient, oxidized FAD. The resulting negative charge at the N5 atom of the flavin system is neutralized by a proton provided by either His149 (DepH) or an adjacent water molecule (GliT/HlmI; Figure 1B, Figure 3, and Figure S2 in the Supporting Information), which is preoriented by Asp149OD2/His149NE2, His54O, and the O4 and N5 atoms of FAD. As in TrxR,[11] mutation of aspartic acid 149 to either Asn or Ala completely inactivates GliT (Figure 2B), indicating that aspartic acid 149 protonates the N5 atom of the cofactor via the above-mentioned water molecule and hereby activates the FAD. In addition, the positive pole of helix H8, pointing onto the O2 atom of the cofactor, reinforces the electron-withdrawing effects of the flavin moiety.[11,15] Transfer of the second electron from Cys148SG to FADH prompts the N1 atom of the prosthetic group to grab the proton of the substrate's second thiol. By a concerted cascade of electron-pair shifts the disulfide-bridged natural product is formed and the oxidized state of the CXXC box is restored. In the final reaction step GliT and HlmI use their gained reductive equivalents to produce H_2O_2 from O_2.[8a,9a] By contrast, $FADH_2$ in DepH donates the electrons to $NADP^+$.[9b] The reduction of $NADP^+$ is assumed to require structural rearrangements as in TrxR.[11,16]

Substrate binding in GliT, HlmI, and DepH may involve Arg48 and His144. Noteworthy, the orientation of Arg48 is identical in all three enzymes and its mutation to Ala impairs GliT's activity. His144 adopts distinct conformations in GliT, HlmI, and DepH, and its replacement by either Ala or Asn severely reduces the catalytic activity (Figure 1B and Figure 2B). Initial deprotonation of the substrate may be triggered by His144 and by the positive N-terminal dipole of the CXXC helix H4 (Figure 3). Evidence for the relevance of this helix dipole is provided by a water molecule occupying the center of the helix bottom in the GliT and DepH apo structures (Figure 1B). The active site of HlmI shows strong additional positive electron density, which in agreement with mass spectrometric analysis has been interpreted as a GSH molecule covalently bound to Cys145 (Figures S4 and S5 in the Supporting Information). As the ligand is only poorly defined in the $2F_O-F_C$ electron density map, its occupancy has been set to 0.5. Remarkably, the thiol of GSH occupies the position of the water molecule in GliT and DepH and is thus perfectly aligned with the positively charged H4 helix dipole (Figure S5C in the Supporting Information). This arrangement facilitates deprotonation of the substrate by lowering its pK_a value and stabilizes the resulting negative charge for the subsequent nucleophilic attack on the enzyme's disulfide. Unlike natural substrates, GSH lacks the second thiol that is required to resolve the enzyme–ligand complex. Consequently, the negative charge is captured at Cys148. In agreement, the distance between Cys148SG and the $C4^{\alpha}$ of FAD in GSH-bound HlmI is shorter (3.1 Å) than that in the

nonliganded structures GliT and DepH (3.4 Å; Figure 1 B and Figure S5 in the Supporting Information).

Even though GliT, HlmI, and DepH employ identical reaction mechanisms to oxidize thiols, their substrate-binding clefts and specificities differ substantially (Figure 1 C). The sizes of the natural substrates **5** and **6** conform to the narrow active-site cavity of HlmI and the spacious pocket of DepH, respectively. However, in comparison to **4**, the rather large pocket of GliT might confer broad substrate specificity. For instance, GliT has been shown to cross-react with **5**,[9a] making it attractive for protein-engineering attempts. In contrast, **4** is converted solely by GliT (Figure 2 D,E), implying that it may not fit into HlmI and may not be properly stabilized in DepH.

In conclusion, the disulfide-forming flavoenzymes GliT, HlmI, and DepH are engaged in highly diverse biosynthetic pathways across unrelated microbial kingdoms. Despite marked differences in their substrate specificity, they share a common reaction mechanism. These traits may be employed to tailor oxidoreductases for biocatalytic applications. In addition, the presented X-ray structures may also set the basis to establish GliT from *A. fumigatus* as a novel drug target for the treatment of invasive aspergillosis and to promote the design of selective inhibitory compounds for this type of oxidoreductases.

Received: October 24, 2013
Published online: January 20, 2014

Keywords: disulfide bonds · enzyme catalysis · natural products · oxidoreductases · sulfur

[1] T. R. Dagenais, N. P. Keller, *Clin. Microbiol. Rev.* **2009**, *22*, 447 – 465.
[2] K. J. Kwon-Chung, J. A. Sugui, *Med. Mycol.* **2009**, *47, Suppl. 1*, S97 – 103.
[3] D. M. Gardiner, P. Waring, B. J. Howlett, *Microbiology* **2005**, *151*, 1021 – 1032.
[4] D. H. Scharf, T. Heinekamp, N. Remme, P. Hortschansky, A. A. Brakhage, C. Hertweck, *Appl. Microbiol. Biotechnol.* **2012**, *93*, 467 – 472.
[5] a) C. J. Balibar, C. T. Walsh, *Biochemistry* **2006**, *45*, 15029 – 15038; b) R. A. Cramer, Jr., M. P. Gamcsik, R. M. Brooking, L. K. Najvar, W. R. Kirkpatrick, T. F. Patterson, C. J. Balibar, J. R. Graybill, J. R. Perfect, S. N. Abraham, W. J. Steinbach, *Eukaryotic Cell* **2006**, *5*, 972 – 980.
[6] D. H. Scharf, N. Remme, A. Habel, P. Chankhamjon, K. Scherlach, T. Heinekamp, P. Hortschansky, A. A. Brakhage, C. Hertweck, *J. Am. Chem. Soc.* **2011**, *133*, 12322 – 12325.
[7] a) D. H. Scharf, P. Chankhamjon, K. Scherlach, T. Heinekamp, M. Roth, A. A. Brakhage, C. Hertweck, *Angew. Chem.* **2012**, *124*, 10211 – 10215; *Angew. Chem. Int. Ed.* **2012**, *51*, 10064 – 10068; b) D. H. Scharf, P. Chankhamjon, K. Scherlach, T. Heinekamp, K. Willing, A. A. Brakhage, C. Hertweck, *Angew. Chem.* **2013**, *125*, 11298 – 11301; *Angew. Chem. Int. Ed.* **2013**, *52*, 11092 – 11095.
[8] a) D. H. Scharf, N. Remme, T. Heinekamp, P. Hortschansky, A. A. Brakhage, C. Hertweck, *J. Am. Chem. Soc.* **2010**, *132*, 10136 – 10141; b) M. Schrettl, S. Carberry, K. Kavanagh, H. Haas, G. W. Jones, J. O'Brien, A. Nolan, J. Stephens, O. Fenelon, S. Doyle, *PLoS Pathog.* **2010**, *6*, e1000952.
[9] a) B. Li, C. T. Walsh, *Biochemistry* **2011**, *50*, 4615 – 4622; b) C. Wang, S. R. Wesener, H. Zhang, Y. Q. Cheng, *Chem. Biol.* **2009**, *16*, 585 – 593.
[10] D. Mustacich, G. Powis, *Biochem. J.* **2000**, *346 Pt 1*, 1 – 8.
[11] G. Waksman, T. S. Krishna, C. H. Williams, Jr., J. Kuriyan, *J. Mol. Biol.* **1994**, *236*, 800 – 816.
[12] P. A. Karplus, G. E. Schulz, *J. Mol. Biol.* **1987**, *195*, 701 – 729.
[13] C. Thorpe, C. H. Williams, Jr., *J. Biol. Chem.* **1976**, *251*, 3553 – 3557.
[14] a) E. J. Heckler, P. C. Rancy, V. K. Kodali, C. Thorpe, *Biochim. Biophys. Acta Mol. Cell Res.* **2008**, *1783*, 567 – 577; b) C. Thorpe, K. L. Hoober, S. Raje, N. M. Glynn, J. Burnside, G. K. Turi, D. L. Coppock, *Arch. Biochem. Biophys.* **2002**, *405*, 1 – 12.
[15] A. Mattevi, A. J. Schierbeek, W. G. Hol, *J. Mol. Biol.* **1991**, *220*, 975 – 994.
[16] B. W. Lennon, C. H. Williams, Jr., M. L. Ludwig, *Science* **2000**, *289*, 1190 – 1194.

